Photochemistry and Photobiology, 2012, 88: 1217–1226

Proteomic Profiling of the Photo-Oxidation of Silk Fibroin: Implications for Historic Tin-Weighted Silk

Caroline Solazzo*[1,2], Jolon M. Dyer[2,3,4], Santanu Deb-Choudhury[2], Stefan Clerens[2] and Paul Wyeth[5]

[1]BioArCh, Department of Archaeology, University of York, York, UK
[2]Proteins and Biomaterials, AgResearch Lincoln Research Centre, Christchurch, New Zealand
[3]Biomolecular Interaction Centre, University of Canterbury, Canterbury, New Zealand
[4]Riddet Institute at Massey University, Palmerston North, New Zealand
[5]Cherish Consultancy, Winchester, UK

Received 25 January 2012, accepted 18 April 2012, DOI: 10.1111/j.1751-1097.2012.01167.x

ABSTRACT

The stability of silk proteins to ultraviolet light is an issue of significant concern in both the appearance retention of silk-derived products and the preservation of historic silk textiles. Until now, evaluation of silk degradation has only been performed at the holistic, rather than molecular level. This article describes the first proteomic profiling of silk photo-oxidation, characterizing protein primary level modification leading to coloration changes, and evaluating the effects of tin weighting on photodegradation. Heavy-chain fibroin, the main proteinaceous component of the silk thread, is a repetitive, highly crystalline protein with a content rich in tyrosine. Photoproducts of tyrosine were characterized and the levels of oxidative modification at the protein primary structural level correlated with changes in coloration and tensile strength. The effect of tin as a weighting agent used on historical fabrics was examined. Tin-weighted fabrics were evaluated following two treatments (pink and dynamite) and proteomic analysis revealed a significant increase in oxidatively modified amino acid residues within the pink-treated silk. These findings offer new insight into the molecular-level oxidation of silk proteins under UV exposure, and the effects of silk treatments in either exacerbating or ameliorating this degradation.

INTRODUCTION

Silk has a long and important place in the history of textile production, and retains today the status of a luxury fiber (1,2). A natural fiber, under certain conditions it is susceptible to rapid physical and chemical changes. Photodegradation is a major issue that affects textiles during aging: fabrics made of protein fibers, such as wool and silk tend to discolor when exposed to UV light. Preventing the photoyellowing of modern fabrics is critical for obvious commercial interests. The problem is even more significant for historical textiles that have been exposed to UV light during their lifetime or during display in museums (3,4). Photodegradation of silk not only leads to an ''irreversible'' change of color but also affects other physical properties of the fabric, such as strength and elasticity. Understanding the mechanisms that lead to the photodegradation of silk is one step to offer better methods to prevent or mitigate the degradation of silk.

Silk is an extracellular proteinaceous fiber produced primarily from the domesticated silkworm *Bombyx mori*. The fiber reeled from the cocoon comes as a thread made of highly crystalline and insoluble proteins, the fibroins, glued with sericin, an amorphous protein. The series of treatments that create the end product of silk generate damage to the fiber. The main process is the degumming of the fiber or the silk fabric to remove the sericin and make the fiber lustrous. This is usually carried out by boiling at high temperature, with or without the addition of chemicals (salts or detergents, [4,5]). The weight lost during degumming was in the past replaced by organic compounds, such as glues, waxes or sugars and later on by metal agents, essentially tin, iron and lead. Metal weighting became the most common method from the late 18th century to the early 20th century, in particular with tin salts, as it enhanced some qualities in the fabric: weight, thickness and better draping (6). However, the susceptibility to degradation, and photodegradation in particular, is increased for silk fabrics weighted with some metal salts, which has resulted in poorly preserved historical textiles. Previous studies have shown that weighting and UV aging resulted in loss of strength (7–10), due to the disorientation of the crystallites in the fibroin chains and the shortening of the fibroin polymer (11,12). Exposure to light leads to hydrolytic and oxidative damage, which are believed to happen first in the amorphous regions (3,4,8,11). Such damage includes protein chain scission, cross-links or amino acid residue side-chain modifications (12). Amino acid analysis have also indicated a loss of tyrosine under UV light aging with mol% of degummed silk changing from 5.1 to 3.3 (13).

Herein, we examine molecular modification at the protein residue level using the approach of enzymatic digestion of silk with subsequent mass spectrometric-based evaluation. The selected proteomic methodology was expected to better characterize the types and sites of modifications than more traditional holistic methods of analysis, and help build a more accurate model of silk photodegradation from the molecular level up. Recent advances in the area of evaluating wool photoyellowing have demonstrated the potential advantages of using, such an approach (14–16). Silk is a particularly susceptible fiber to UV-induced coloration changes as it is

*Corresponding author email: solazzo.c@gmail.com (Caroline Solazzo)

rich in tyrosine (5% of the total heavy chain), which (together with tryptophan and phenylalanine, [17,18]) is one of the key amino acids responsible for protein photoinduced discoloration (in wool, skin, hair and food). The composition (19) and structure (20,21) of silk have been well characterized, facilitated by the full sequencing of the L-chain (22), H-chain (23,24), and of the *B. mori* genome in 2004 (25,26), allowing the development of proteomics studies (27) on silkworm (28,29), silk gland (19,27,30) and silk proteins (31,32). The main proteins of silk, the fibroins, come in two forms: the light chain (L-chain), a short protein of 262 residues, and the heavy chain (H-chain), a long protein of 5263 residues, made of many repetitive fragments. The high crystallinity and therefore strength of silk is due to the presence in the H-chain of residues with small side-chains, glycine (46%), alanine (30%) and serine (12%), forming the hexapeptide repeat Gly–Ala–Gly–Ala–Gly–Ser (GAGAGS). The tyrosine(Y)-containing blocks (such as GAGAGY or GAGAGVGY) form semicrystalline regions. The H-chain is thus made of 12 hydrophobic crystalline regions (∼GAGAGS∼/∼GY∼∼∼GY∼) separated by 11 amorphous hydrophilic regions (∼GT∼∼∼GT∼) containing residues with large side-chains (24,33,34), and hydrophilic head and tail regions (20). These amorphous regions form turns resulting in an antiparallel β-pleated sheet secondary structure (21) where protein chains are held together by noncovalent interactions, notably hydrogen bonding. The H-chain is linked to the small globular L-chain fibroin by a disulfide bridge between Cys-20 (H-chain) and Cys-172 (L-chain; 22,34–36). Finally, a glycoprotein (P25) completes the fibroin structural arrangement, incorporated once in every six H-chain-L-chain dimers through hydrophobic interactions (37). The role of the glycosylated protein is to maintain the structure of the H–L unit, preventing denaturation (32,35).

Silk is insoluble in water, but can be dissolved in concentrated organic salts solutions (38). We used the aqueous calcium chloride–ethanol system (39–41) to dissolve degummed silk and tin-weighted silk before and after UV aging. Enzymatic digestion was performed with chymotrypsin, proven to be the most efficient enzyme for in-gel digestion of the three silk proteins (31). It has high-proteolytic specificity in cleaving peptide bonds at the C-termini of tyrosine, tryptophan and phenylalanine, and to some extent leucine, methionine, alanine, aspartic and glutamic acids. It is best suited for the digestive generation of peptides from the heavy chain of silk fibroin, which is particularly rich in tyrosine with 277 residues in total. Liquid chromatography coupled to mass spectrometry (LC–MS) was utilized to characterize photo-oxidative modifications within fibroin peptides (MS/MS), locate the sites within the primary structure, and profile the extent of photo-oxidation using a previously established redox proteomic scoring system (16).

MATERIALS AND METHODS

Silk and fabric preparation. Undyed, plain-weave silk fabric (Whaleys habotai silk, 40 g m^{-2}; thread count per cm: warp 147, weft 122) was degummed in a 1% sodium dodecylsulfate + 1% sodium carbonate solution for 1 h at 98 ± 2°C, rinsed thoroughly in purified water and dried at room temperature. The fabric was then cut into 25 mm wide strips along the warp for artificial aging.

Silk weighting. Plain weave, degummed, undyed silk samples (yarn count: warp 25, weft 45, 34 g m^{-2}) were weighted using two methods—"pink" tin (Sn[IV] chloride and sodium phosphate; three repetitions; weight gain 54%) and "dynamite" tin (Sn[IV] chloride, sodium phosphate, sodium silicate and aluminium sulfate; two repetitions; weight gain 98%). In the text, samples will be referred as: SU and SA for degummed unweighted silk, unaged and aged; PU and PA as pink tin-weighted silk, unaged and aged; and DU and DA as dynamite tin-weighted silk, unaged and aged.

Irradiation protocols. The surrogate materials were subjected to accelerated aging. Light aging was carried out in a Q-Sun "Xe1 Xenon Test Chamber" (Q-Lab, Westlake, OH) for 1 week; the temperature was maintained at 28°C, and the system was programed to deliver 0.4 W m^{-2} of light energy at the wavelength 340 nm (equivalent to a total dose of 25 MJ m^{-2} over 1 day). The positions of the samples were rotated regularly to ensure even exposure.

Color analysis. Color measurements in the CIE-XYZ color space were taken using a Minolta Chroma Meter CR200 (Konica Minolta Optics, INC., Tokyo, Japan) with an 8 mm diameter measuring area, 10º viewing angle and diffused illumination. Each color measurement represented the average of three readings.

Tensile tests. Mechanical testing was carried out on test strips of dimension 2.5 × 5 cm, using an Instron "5544" (Instron RX 5544, Machine Solutions Inc. (MSI), Flagstaff, AZ) instrument controlled by "BLUEHILL" software (Bluehill(R)software from Instron Pty Ltd., Melbourne, Australia); a gauge length of 3 cm and extension rate of 2 mm min^{-1} were employed, and the samples tested to breaking point. Six replicates for each sample were assessed (those which broke at the jaw were excluded, and it was ensured that there were at least four valid replicates in every group); average values (and SDs) were calculated for each set. Samples were equilibrated at 20 ± 2°C and 55 ± 5% relative humidity for at least 72 h prior to testing, and these conditions were also maintained throughout the experiment.

Chemicals. Calcium chloride ($CaCl_2$) and α-chymotrypsin were provided by Sigma–Aldrich (St. Louis). Triethylamine (TEA) was provided by Acros Organics (New Jersey), phenyl isothiocyanate (PITC) by Fluka Biochemika (Sigma–Aldrich, Austria), sodium acetate trihydrate by Merck (Germany), sodium azide by AnalaR NORMAPUR (VWR, Prolabo, Leuven), Ethylenediaminetetraacetic acid (EDTA) by J. T. Baker (USA), disodium hydrogen phosphate (Na_2HPO_4) by BDH AnalaR® (UK) and the Pierce Amino Acid standard H by Thermo Scientific (Rockford, IL). Methanol (MeOH) was provided by Scharlau (Spain), ethanol (EtOH) by Fisher Scientific (Loughborough, UK), acetonitrile (ACN) and water (H_2O) by Fisher Scientific (Fair Lawn), hydrochloric acid (HCl) by MERCK (Germany) and formic acid (FA) by Ajax Finechem Pty Ltd (Univar® analytical reagents), Thermo Fisher Scientific (Auckland, NZ).

Digestion. The silk fabrics were ground in liquid nitrogen and reduced to a fine powder let to dry overnight. Two samples of 1 mg each were weighed to run duplicates of each fabric and samples were solubilized at 75°C for 1 h in 0.5 mL of a solution of $CaCl_2$/EtOH/H_2O (111/92/144 in weight) according to the Ajisawa method (39,42). The extracts were then dialyzed in water with 3500 MWCO dialysis filters (Thermo Scientific, Rockford, IL), changing the water every day. After 3 days, they were concentrated on a vacuum centrifuge for 2 h and digested for 18 h at 37°C with 50 μg of chymotrypsin in 100 μL of peptide digestion buffer prepared from a two-fold dilution of chymotrypsin solution (chymotrypsin in $CaCl_2$/1 mM HCl buffer) in 100 mM Tris/10 mM $CaCl_2$ adjusted to pH 7.8. Samples were centrifuged and the supernatant dried down and diluted before analysis in ACN solution with 0.2% FA for a final concentration of 1:1000.

LC-MS/MS evaluation. LC–MS/MS was carried out on an Ultimate nanoflow HPLC equipped with Famos autosampler and Switchos column switching module (LC-Packings, The Netherlands). A 10 μL sample was loaded on a C18 precolumn (Varian Microsorb 300 μm ID, 5 μm particles, 300 Å pore size) at a flow rate of 8 μL min^{-1}. The precolumn was then switched in line with the analytical column (Microsorb C18, 20 cm, 75 μm ID, 5 μm particles, 300 Å pore size), and eluted at a flow rate of 150 nL min^{-1}, with a gradient from 2% to 55% B in 50 min. Solvent A was HPLC-grade H_2O with 0.2% FA, solvent B was LCMS-grade ACN with 0.2% FA. Using a stainless steel nanospray needle (Proxeon, Denmark), the column outlet was directly connected to a QSTAR Pulsar i mass spectrometer (Applied Biosystems), which was programed to acquire MS/MS traces of 1+, 2+, 3+, 4+ and 5+ peptides in three simultaneous MS/MS.

Bioinformatic analysis.Mascot Daemon (Matrix Science, UK) was used to extract peak lists from the LC–MS/MS data files. The peak lists from all *m/z* segments of each sample were concatenated and imported in Protein-Scape v2.1 (Bruker daltonics). Subsequently, Mascot was used to search for matches with known silk sequences, grouped in a database under the *Bombyx* taxonomy.

Amino acids analysis.Ground silk samples were weighed in glass tubes and placed in a reaction vial containing 400 μL of 6 *N* HCl and a crystal of phenol. L-norleucine was added as an internal standard in each sample. The samples were hydrolyzed for 20 h at 110°C after flushing with N_2 under vacuum. After hydrolysis, the samples were dried at 55°C, 25 μL of H_2O/MeOH/TEA (2:2:1) mixture was then added to the samples, vortexed thoroughly and dried again. The samples were then resolubilized in 200 μL of 5 mM of Na_2HPO_4 (pH 7.4) and filtered through cellulose acetate 0.45 μm filters. Standards were prepared containing a mix of cysteic acid, lysinoalanine, lanthionine, L-norleucine and Pierce AA standards at final concentration of 1.25 nmol, 7.5 nmol and 12 nmol. A 10 μL of each sample was derivatised with a solution of MeOH/H_2O/PITC/TEA (17/1/1/1 in volume) for 20 min at room temperature. After drying at 55°C, the derivatised samples were resolubilised in 400 μL of 5 mM of Na_2HPO_4 (pH 7.4).

Triplicate analysis was performed on a Dionex Ultimate 3000 HPLC (Dionex Softron GmbH, Germany) equipped with an autosampler (Dionex Softron GmbH) and photodiode array detector (Dionex Softron GmbH); the software used was CHROMELEON™ version 6.80 (Thermo Fisher Scientific Inc., Sunnyvale, CA). A 20 μL sample was loaded on a SB-C18 column (Agilent Zorbax 5 μm ID, 4.6 × 250 mm, 3.5 μm pore size) heated at 40°. An initial 5 min equilibration at 98% A and 2% B was followed by a tailored 60 min gradient at a flow rate of 1 mL min^{-1}. Mobile phase A contained 140 mM sodium acetate, 15 mM sodium azide, 0.1% EDTA and 0.05% TEA titrated to pH 5.9 using acetic acid. Mobile phase B was ACN and mobile phase C was MeOH.

RESULTS AND DISCUSSION

Proteomic evaluation

LC–MS/MS evaluation was performed after chymotryptic digestion of the silk. No enzyme was specified in the search parameters so as to allow for parallel identification of both chymotryptic peptides as well as nonenzymatic protein backbone cleavages that can occur during photo-oxidation. Mass tolerances were set at a peptide mass tolerance of 100 ppm and a fragment mass tolerance of 0.2 Da. Previous studies have shown that the aromatic residues, in particular, are sensitive indicators of protein oxidative damage, and these are also strongly implicated in the photoinduced discoloration of protein materials, notably photoyellowing. On the basis of reported photomodifications to aromatic amino acid residues (14,15,43,44), single and double oxidation on aromatic residues (tyrosine, tryptophan and phenylalanine), quinone and hydroxyquinone (oxidized tyrosine) were chosen as variable modifications. In addition, N-terminal acetylation, C-terminal amidation and methylation, deamidation (N and Q), oxidation of methionine and phosphorylation (S, T and Y) were added as variable modifications. Peptides with a Mascot MS/MS score of greater than 28 were prescreened for further evaluation and subsequently validated through manual analysis of the MS/MS data. MS/MS spectra with little y or b fragment ion sequence coverage were removed from evaluation. All validated peptide data are compiled in Table S1 (Supporting information; unaged samples) and Table S2 (aged samples). As a general observation, Mascot-identified peptides with hydroxylation type oxidative modifications were observed to have a lower score than other types of modification. Examination of the spectra for such modified peptides suggested that this is due to secondary fragmentation peaks from hydroxylated fragments (loss of 16, 18 etc.) that lower the intensity of the more standard fragment ions.

Protein characterization. SM1 and 2 give the identified proteins with their accession number, percentage coverage, identified peptides and modifications for each fabric type (samples run in duplicates). Chymotrypsin digestion resulted in high-sequence coverage for the light-chain (up to 81%) and the heavy-chain fibroin (up to 14% or 77% when considering the large number of homologous peptides repeated throughout the protein sequence). In addition, P25 was identified, albeit with relatively low-sequence coverage, possibly due to the low abundance of the protein. At least two isoforms of the light chain were identified (see SM), the differences appearing at positions 80, 123, 145 and 183 and are respectively found as P80, I123, T145 and S183 in gi|24637964, and S80, R123, I145 and G183 in gi|19221230. The main hit for the heavy-chain was gi|164448672, but peptides from the incomplete gi|765323 protein were occasionally identified, suggesting the presence of a second isoform for the heavy chain too.

The high number of chymotryptic cleavages sites (mainly tyrosine and alanine) resulted in a large variety of digested fragments in the heavy-chain fibroin (45). The reported total number of identified peptides in the unaged silk is similar for the three fabrics at 96 for SU, 102 for PU and 104 for DU. The dataset includes many nonchymotryptic peptides (28% in SU, 32% in PU and 36% in DU) at percentages that remain relatively constant in the aged samples (31% in SA, 37% in PA and 28% in DA), likely from photoinduced backbone cleavage or hydrothermally induced protein hydrolysis (38) resulting from degumming at 100°C. Noticeably, the total number of identified peptides in the dynamite tin-weighted samples drops to 70 after UV irradiation (33% decrease). In comparison, the total number of peptides in the unweighted samples increases to 138 (30% increase), and in the pink tin-weighted samples to 114 (12% increase). The heavy-chain fibroin percentage coverage is consequently increased in these two cases, whereas it decreases in the dynamite tin-weighted sample. The solubility and digestibility of silk might be facilitated in the unweighted aged sample by a loss of crystallization of the heavy-chain. This is less evident in the pink tin-weighted silk, whereas the loss of observed peptides in the dynamite tin-weighted silk might be a consequence of large amount of tin added in the weighting process. Digestibility is also expected to be altered by photoinduced cross-linking, and it is possible that differential amounts of such cross-links are being formed between these samples.

Deamidation was also observed as a frequent modification in the light-chain fibroin, which has a higher proportion of glutamine and asparagine residues than the heavy chain. Weighting and aging of the silk fabric was not observed to induce an increase in the level of deamidation.

Photomodifications. A summary of the oxidatively modified peptides observed in the light and heavy-chain fibroins for all samples is shown in Table 1. Specifically, peptide *m/z*, the peptide sequence, the position(s) in the protein, the modification type and position in the peptide and the relative degree of oxidative modification are reported for each peptide.

Table 1. Oxidised peptides in silk fabrics before and after UV aging.

Observed *m/z*	Sequence	Position in the protein chain	Photomodification (s): position*	Protein	p	P
SU						
576.2922	L.NVQEILKDMASQGDY.A	61–75	M9 → [M + O]	LC	1	1
708.860	L.MKTLSDGTVAQSY.V	103–115	M1 → [M + O]	HC	1	1
647.300	Y.GAASGAGAGAGAGAGAGYGTGAGAG.A	172–196	Y18 → [Y + O]	HC	1	1
658.309	G.AGAGSGAGVGYGAGVG.A	621–636/919–934/1578–1593	Y11 → Quin	HC	3	9
1013.483	Y.GAGAGAGYGVGY.G	3416–3427	Y8 → Quin	HC	3	3
Total oxidation score					9	15
SA						
754.304	Y.DFEAAW.D	168–173	W6 → [W + O]	LC	1	1
814.929	D.VLMKTLSDGTVAQSY.V	101–115	M3 → [M + O]†	HC	2	2
647.820	A.ASGAGAGAGAGAGAGYG.T	174–190	Y16 → HQuin†	HC	8	8
999.465	A.GAGSGAGAGSGTGAGSGAGAGYGAGAGA.G	462–489	Y22 → [Y + O]†	HC	2	2
1013.473; 507.240	A.GAGYGAGAGVGY.G	550–561/3173–3184/3847–3858/ 3917–3928/3997–4008/4422–4433/ 4663–4674/4763–4774/4849–4860	Y4 → Quin†	HC	6	54
649.321	S.GAGAGVGYGAGAGVGY.G	844–859	Y8 → Quin	HC	3	3
650.306	S.GAGAGVGYGAGAGVGY.G	844–859	Y8 → [Y + O]	HC	1	1
649.318	A.GYGVGYGAGAGAGY.G	1786–1799/2803–2816/2887–2910/ 2963–2976/3410–3423/3422–3435/ 3494–3507/3578–3591/3654–3667/ 3754–3767	Y2, Y14 → [Y + 2O]	HC	4	40
708.3358	Y.GAGAGAGVGYGAGAGAGY.G	315–332‡	Y10 → [Y + 2O]	HC	2	2
Total oxidation score					29	113
PU						
814.973	D.VLMKTLSDGTVAQSY.V	101–115	M3 → [M + O]	HC	1	1
708.850	L.MKTLSDGTVAQSY.V	103–115	M1 → [M + O]	HC	1	1
649.358	S.GAGAGVGYGAGAGVGY.G	844–859	Y8 → Quin	HC	3	3
999.521	A.GAGYGAGVGAGYGAAYGAGAGAGY.G	1891–1914	Y16 → [Y + 2O]	HC	2	2
1013.512	Y.GAGAGAGYGVGY.G	3416–3427	Y8 → Quin	HC	3	3
Total oxidation score					10	10
PA						
814.394	D.VLMKTLSDGTVAQSY.V	101–115	M3 → [M + O]	HC	1	1
647.789	A.ASGAGAGAGAGAGAGYG.T	174–190	Y16 → [Y + O]	HC	1	1
709.312	A.GAGAGAGYGTGAGAGAGA.G	182–199	Y8 → HQuin	HC	4	4
909.413	A.GAGAGTGAGAGYGAGAGAGAGAGY.G	300–323	Y12 → [Y + 2O] Y24 → [Y + O]	HC	3	3
708.300	A.GAGTGAGAGYGAGAGAGAGAGYGAASGTGAGYGA.G	302–335	Y10 → HQuin; Y22, Y32 → [Y + 2O]	HC	8	8
850.361	G.AGTGAGAGY.G	303–311	Y9 → [Y + 2O]	HC	2	2
1013.428	A.GAGYGAGAGVGY.G	550–561/3173–3184/3847–3858/ 3917–3928/3997–4008/4422–4433/ 4663–4674/4763–4774/4849–4860	Y4 → Quin	HC	3	27
649.299	S.GAGAGVGYGAGAGVGY.G	844–859	Y8 → Quin	HC	3	3
659.626	S.GAGAGSGAGYGAGVGAGYGAGYG.A	1277–1299	Y10 → [Y + O]; Y22 → [Y + 2O]; Y18 → HQuin	HC	7	7

Table 1. (Continued)

Observed *m/z*	Sequence	Position in the protein chain	Photomodification (s): position*	Protein	p	P
752.865	G.AGSGAGAGSGAGAGYGAGY.G	1356–1374/1504–1522/ 1677–1695/2252–2270/ 2433–2451/3150–3168/ 3824–3842/3974–3992/ 4399–4417/4487–4505/ 4640–4658/4740–4758/ 4914–4932	Y19 → [Y + 2O]; Y15 → Quin	HC	5	65
708.3	V.GAGYGAGYGAGAGAGYGAGAGSGTG.S	2352–2376	Y8 → Quin	HC	3	3
1013.437	S.GAGAGYGVGYGA.G	2883–2894/3418–3429/ 3574–3585	Y6 → Quin	HC	3	9
816.364	S.GAGAGYGVGYGAGAGAGYGA.G	2883–2902/3418–3437/ 3574–3593	Y18 → Quin	HC	3	9
999.444	G.SGAGAGAGAGAGAGSGAGAGSGAGAGYG.A	5088–5115	Y27 → [Y + 2O]	HC	2	2
708.300	Y.GAGAGAGVGYGAGAGAGY.G	315–332‡	Y10 → [Y + 2O]	HC	2	2
Total oxidation score					50	146
DU						
708.834	L.MKTLSDGTVAQSY.V	103–115	M1 → [M + O]	HC	1	1
814.951	D.VLMKTLSDGTVAQSY.V	101–115	M3 → [M + O]	HC	1	1
649.344	S.GAGAGVGYGAGAGVGY.G	844–859	Y8 → Quin	HC	3	3
909.446	G.AGAGSGAGAGSGAGAGYGAGYGAG.A	112–135‡	Y15 → [Y + O]; Y21 → HQuin	HC	5	5
752.722	A.FGAGAGAGAGSGAGAGSGA.G	2407–2425	F1 → [F + 2O]	HC	2	2
837.388	A.WSSESDFGTGSGAGAGSGAGAGSGAGAGY.G	3810–3838/4201–4229/4548–4576	F7 → [F + 2O]	HC	2	6
Total oxidation score					14	18
DA						
814.920	D.VLMKTLSDGTVAQSY.V	101–115	M3 → [M + O]	HC	2	2
850.382	G.TGAGAGYGA.G	305–313	Y7 → [Y + 2O]	HC	2	2
710.337	T.GAGSGAGAGYGAGAGAGY.G	474–491/528–545/1022–1039/ 1981–1998/2095–2112/ 2203–2220/4099–5016	Y18 → [Y + O]; Y10 → [Y + 2O]	HC	3	21
909.393	S.GAGAGTGAGAGSGAGAGYGAGAGS.G	3211–3234	Y18 → Quin	HC	3	3
648.295	S.GAGAGTGAGAGSGAGAGYGAGAGSG.A	3211–3235	Y18 → [Y + O]	HC	1	1
999.452	S.DFGTGSGAGAGSGAGAGSGAGAGY.G	3815–3838/4206–4229/4553–4576	F2 → [F + O]	HC	1	3
784.366	G.AGAGAGAGSGAGAGSGAGAGYG.A	5094–5115	Y21 → [Y + O]	HC	1	1
918.401	S.GAASGAGAGAGAGTGSSGFGPY.V	5121–5142	Y22 → Quin	HC	3	3
Total oxidation score					16	36

[Y + O], single oxidation; [Y + 2O], double oxidation; Quin, quinone; HQuin, hydroxyquinone; LC, light chain fibroin; HC, heavy-chain fibroin; p is the score of the peptide; P the score in the protein that includes the various repeats of the peptide; *For full reports of modifications, see Tables S1 and S2; †Identified in both duplicates; ‡In gi765323.

In previous studies on protein photoyellowing, tryptophan is the amino acid residue whose modification has been observed to most closely correlate with color formation, but tryptophan is present only in very low-relative abundance in fibroins. Only one oxidized tryptophan (W_{173}) was observed in the light-chain fibroin of the aged unweighted sample (Fig. 1a). Phenylalanine was found oxidized in the heavy-chain in the dynamite tin-weighted sample only: at F_{2407} and F_{3816} in DU (double oxidation) and F_{3816} in DA (single oxidation). Most of the oxidation occurs on the tyrosine residues (Fig. 1b) shows a peptide with double oxidation and Fig. 1c shows a peptide with quinone oxidation).

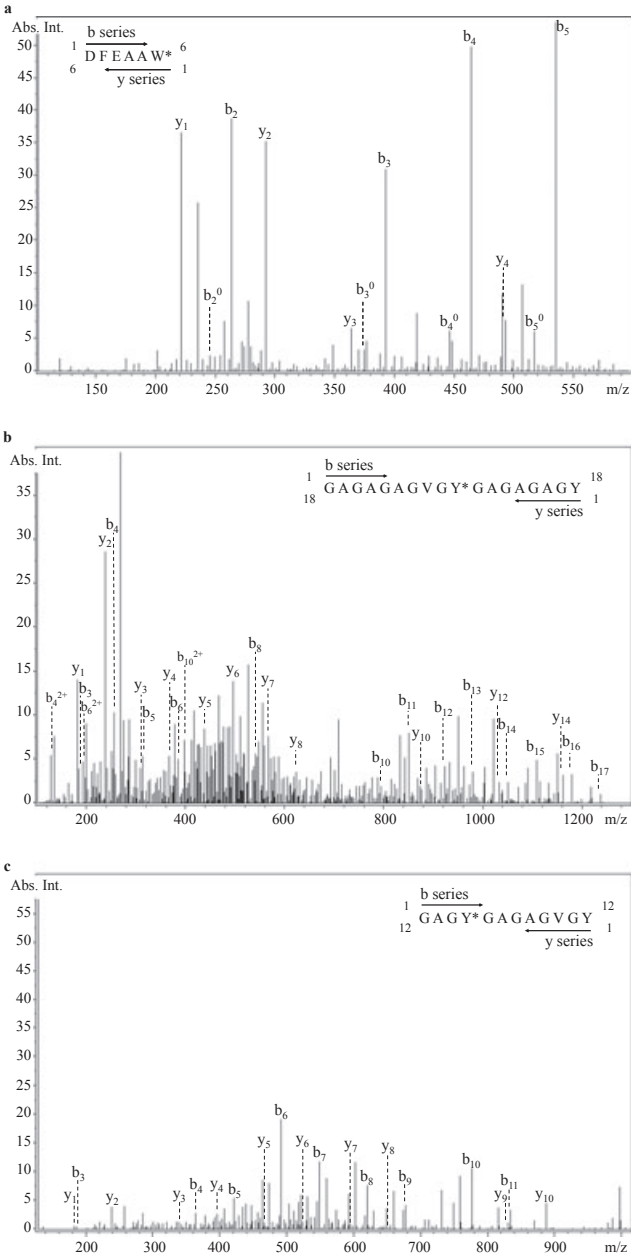

Figure 1. MS/MS spectra of: (a) monocharged peptide DFEAAW, *m/z* 754.304 with single oxidation from SA, (b) doubly charged peptide GAGAGAGVGYGAGAGAGY, *m/z* 708.336 with double oxidation from SA and (c) monocharged peptide GAGYGAGAGVGY, *m/z* 1013.428 with quinone oxidation from PA.

Figure 2 describes the general oxidative pathways observed in the photomodification of tyrosine residues (44). A classification of the degree of oxidative degradation for each modified peptide has been calculated by assigning each individual observed oxidative modification within the peptide a score based on the relative level of the modification within this oxidative cascade. Scores were assigned as 1 for those modifications classified as single oxidation, 2 for double oxidation, 3 for quinone formation and 4 for hydroxyquinone formation (16). The single oxidation by addition of a hydroxyl radical leads to dienone alcohol or dihydroxyphenylalanine (dopa), which in turn can be oxidized to trihydroxyphenylalanine (topa) by addition of another hydroxyl radical (double oxidation). The quinone derivative is the product Y + O–2H from tyrosine and hydroxyquinone either from the hydroxylation of quinone or as a photoproduct of topa. The score given to each modification reflects the relative level of modification with respect to the native residue, with initial oxidation products being further modified themselves in a cascade of degradation.

The total oxidation scores calculated in Table 1 for all proteins are the cumulative result of duplicate runs. The scores are shown at the peptide level (p) and at the protein level (P), counting all the repeated sequences in the protein. All modifications included, the unaged silks were classified as having redox scores of p = 9, P = 15 (SU), p = 10, P = 10 (PU) and p = 14, P = 18 (DU). UV aging resulted in a significant increase in the oxidation score in the unweighted and pink tin-weighted samples with scores of p = 29, P = 113 (SA) and p = 50, P = 146 (PA). However, the increase in the

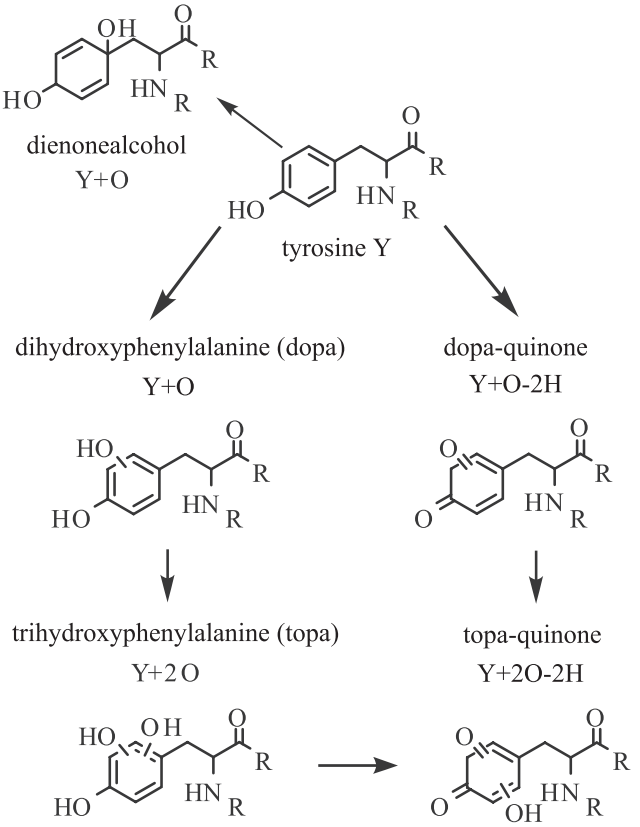

Figure 2. Tyrosine photo-oxidative pathway (44).

dynamite tin-weighted sample is low at scores of p = 16, P = 36 (DA). This result is in line with the decrease in the number of observed fibroin peptides and resultant low-sequence coverage of the heavy-chain fibroin.

Photo-oxidation within the heavy-chain fibroin is playing the predominant role in silk photoyellowing: with 277 tyrosine residues, the protein offers a large choice of oxidation sites. There is a clear increase of all oxidation product types associated with tyrosine in the aged samples, except in the case of hydroxyquinone, which was not observed in the aged dynamite tin-weighted sample.

Color and tensile strength evaluation

Yellowness changes within the silk samples were evaluated by measuring the $\Delta Y–Z$ value on each fabric by comparison with the unaged unweighted fabric. The highest differential value is obtained for the pink tin-weighted sample with an increase of 12 $Y–Z$ units, followed by the dynamite tin-weighted sample with an increase of 9 units. The unweighted sample increases less, by just 6 units, evidence that the tin-weighting process exacerbates silk photoyellowing.

The samples exhibited an exponential correlation between tensile strength and yellowing (R^2 = 0.9863, Fig. 3a). Garside *et al.*, (7,8), conducted tensile strength tests on both tin-weighted and unweighted silks, and concluded that the weighting treatment was causing the loss of tensile strength and not the weighting agent itself. When exposed to artificial light aging, the pink tin-weighted samples were reported to have lower tensile strength, whereas dynamite tin-weighted and untreated silk were less affected. However, the rate of deterioration of pink-treated silk without added tin was comparable to the untreated sample. The study concluded that pink tin-weighted samples were most vulnerable to photodeterioration, and that this susceptibility to light was mediated by the tin itself, as opposed to other components of the weighting process.

In the present study, the protein oxidation score derived from proteomic profiling also shows the highest increase for the irradiated pink tin-weighted sample, following the same trend observed for the tensile strength and yellowing. Figure 3b plots the tensile strength against the total score of oxidation calculated for phenylalanine-, tryptophan- and tyrosine-derived photoproducts, whereas Fig. 3c shows the yellowness $\Delta Y–Z$ against the total score of oxidation. The trendline for SU, PU, SA and PA together exhibits an exponential correlation with a coefficient of correlation of R^2 = 0.9951 (P-values) in Fig. 3b and a linear correlation with a coefficient of correlation of R^2 = 0.9915 (P-values) in Fig. 3c. Although DU plots closely to the trendline, DA is clearly on the outside, showing that the oxidative damage score is likely underestimated only in the aged dynamite tin-weighted silk, consistent with the observed decrease in identified peptides from this sample.

Amino acid analysis

Table 2 gives the composition in amino acids of the silk fabrics in mol%. The mol% of tyrosine and valine are decreased in the unaged samples after the weighting treatment, resulting in an increase in the mol% of glycine and alanine. However, for each

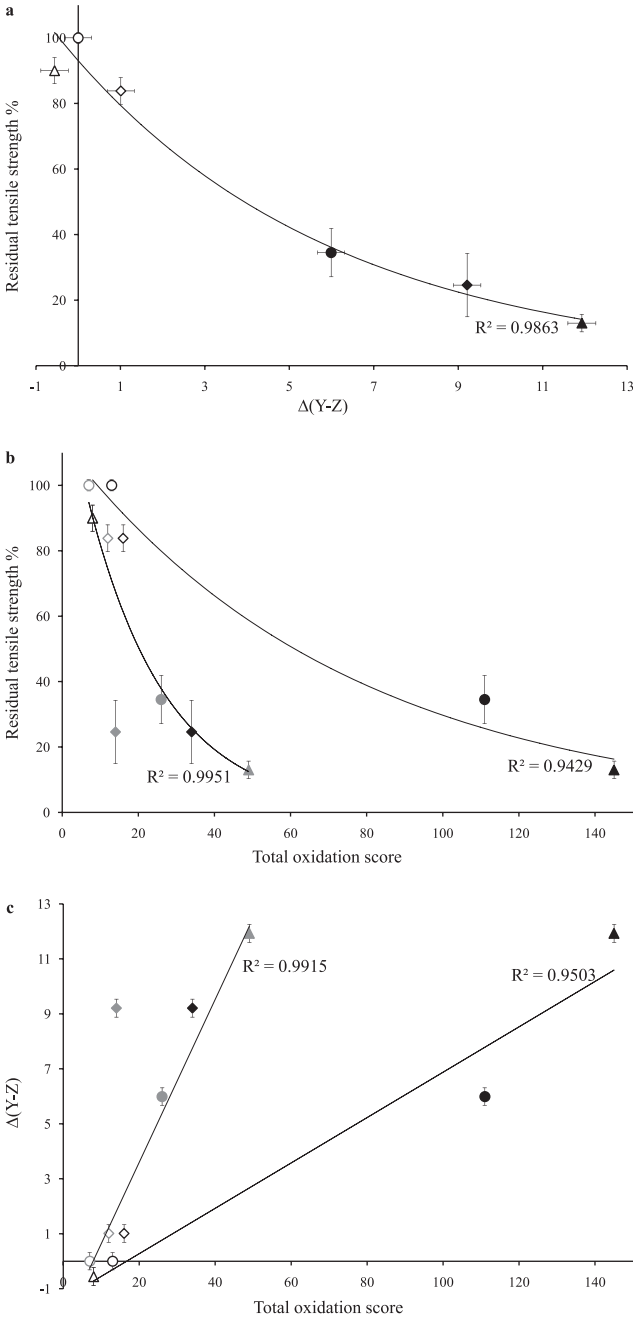

Figure 3. Correlation between: (a) tensile strength and yellowing, (b) tensile strength and score of oxidation products and (c) yellowing and score of oxidation products of unaged samples (open symbols) and aged samples (solid symbols) for unweighted silk (circle), pink tin-weighted silk (triangle) and dynamite tin-weighted silk (diamond). The gray symbols represent the p scores and the black symbols the P scores.

set of samples, only the mol% of tyrosine is decreased after UV aging, from 5.7 ± 0.02 to 4.8 ± 0.01 in the unweighted samples, 5.5 ± 0.02 to 4.6 ± 0.04 in the pink tin-weighted samples and 5.2 ± 0.04 to 4.6 ± 0.03 in the dynamite tin-weighted samples. No decrease is observed for phenylalanine, confirming that tyrosine is the amino acid most affected during photodegradation, as observed before (13). Figure 4a plots the tensile strength against the content of tyrosine in mol% and Fig. 4b the yellowness $\Delta Y–Z$ against the content of tyrosine in

Table 2. Amino acid composition of the silk fabrics in mol%.

Amino acid	SU mol%	SA mol%	PU mol%	PA mol%	DU mol%	DA mol%
Aspartic acid	2.0	2.1	1.8	1.8	1.3	1.3
Glutamic acid	1.0	1.3	1.0	1.1	1.0	0.9
Serine	11.6	11.2	11.5	11.2	11.5	11.3
Glycine	41.7	41.7	42.8	42.3	43.2	43.6
Histidine	0.3	0.3	0.3	0.3	0.3	0.2
Arginine	0.6	0.7	0.5	0.5	0.5	0.5
Threonine	1.1	1.1	1.0	1.0	1.0	0.9
Alanine	29.6	30.3	30.2	31.6	31.2	31.6
Proline	0.5	0.5	0.4	0.5	0.4	0.4
Tyrosine	5.7	4.8	5.5	4.6	5.2	4.6
Valine	2.7	2.8	2.2	2.3	1.9	2.0
Methionine	0.2	0.2	0.2	0.2	0.2	0.2
Cystine	0.1	0.2	0.2	0.2	0.1	0.1
Isoleucine	0.9	0.9	0.8	0.8	0.7	0.7
Leucine	0.7	0.7	0.5	0.6	0.5	0.5
Phenylalanine	0.8	0.9	0.8	0.8	0.7	0.8
Lysine	0.4	0.4	0.4	0.3	0.4	0.3

mol%. As the content of tyrosine decreases, the tensile strength decreases and the yellowing increases, consistent with the previous results showing the increase in oxidation products. The tyrosine oxidation score is plotted against the content of tyrosine in mol% in Fig. 4c, and once again an exponential correlation with a coefficient of correlation of $R^2 = 0.9759$ (P-values) is observed for the unweighted and pink tin-weighted samples plotted together. Although we observe a loss of tyrosine in the dynamite tin-weighted samples, the number of oxidised peptides is underrepresented.

Sites of tyrosine oxidation

Out of the total 277 tyrosine residues in the heavy-chain fibroin, 24 (9%, not including peptide repeats) were observed in an oxidized form within the whole sample set. All but one were found in the crystalline parts of the heavy chain, the exception being a modification observed in the amorphous C-terminal end of the sequence at position 5142. In the crystalline regions, most of the oxidized residues were found in a ~GAGY~ pattern (20), whereas two were found in a ~GVGY~ pattern and one in a ~GAAY~ pattern.

No specific single site was found in an oxidized form in all aged samples. The lack of consistency in the sites of photo-oxidation between samples likely reflects some inherent randomness in the pattern of silk protein photo-oxidation, as well as the low-relative abundance of photosensitive tryptophan residues in fibroin. While it is clear that preferential oxidation occurs in the crystalline regions and in ~GAGY~ patterns, which is a notable result in itself, oxidation sites are well distributed along the protein chain, with only a few sequences that appear regularly oxidized. In this context, it was not possible to identify specific peptide markers of silk photo-oxidation for cross-sample tracking. This is in contrast with the photo-oxidation of other proteinaceous materials, such as wool, where tryptophan oxidation has been observed to occur preferentially at those resides in proximity to another aromatic residue, attributable to energy transfer after photon absorption, and where therefore consistent markers of oxidation can be characterized (14,15). However, utilization of an overarching redox scoring system was able to provide an excellent comparison of molecular-level damage between the samples and gave clear evidence of an increase in photo-oxidized residues throughout the silk due to UV exposure. The extent of protein oxidation is significant when looking at the total peptide score, and correlate nicely with the loss of tyrosine, loss of tensile strength and increase of yellowing. A similar correlation is observed at the protein level when all the potential sites of oxidation are taken into account.

CONCLUSIONS

In this study, a redox proteomic approach was applied for the first time to assess the state of protein oxidative degradation of silk fibroin after light aging, as well as to evaluate the effects of tin weighting on this process. Weighting with tin was a process commonly applied to silk in the past to make up for the loss of weight after degumming. Two processes of tin-weighting were reproduced here: a light (pink) and heavy (dynamite) weighting.

Aromatic residues, which are sensitive indicators of protein oxidation and strongly associated with photoinduced discoloration, were chosen to evaluate overall oxidative degradation (17). In silk proteins, as for collagen (46), tyrosine is present in high-relative abundance, providing many potential oxidation sites on the heavy-chain fibroin. Combined data on tensile strength, color change, amino acid content and protein oxidative modifications show that UV irradiation contributes to a loss of tyrosine through protein oxidation on the tyrosine residues. An increase in yellowing in fibroin was observed to correlate with an increase in the formation of quinone-based tyrosine derivatives. Proteomic profiling of protein damage indicated that the pink tin-weighting process results in high levels of oxidative damage at the molecular level, in addition to significant decreases in whiteness and tensile strength. This was attributed to the presence of tin(IV) oxohydroxide compounds in the pink samples that absorb UV, acting as photosensitisers and thereby increasing susceptibility to sunlight (7). Dynamite tin-weighting, on the other hand, produces sodium tin(IV) aluminophosphosilicate derivatives, which may have less of a photosensitizing effect, although still resulting in higher levels of photoyellowing than for degummed unweighted silk.

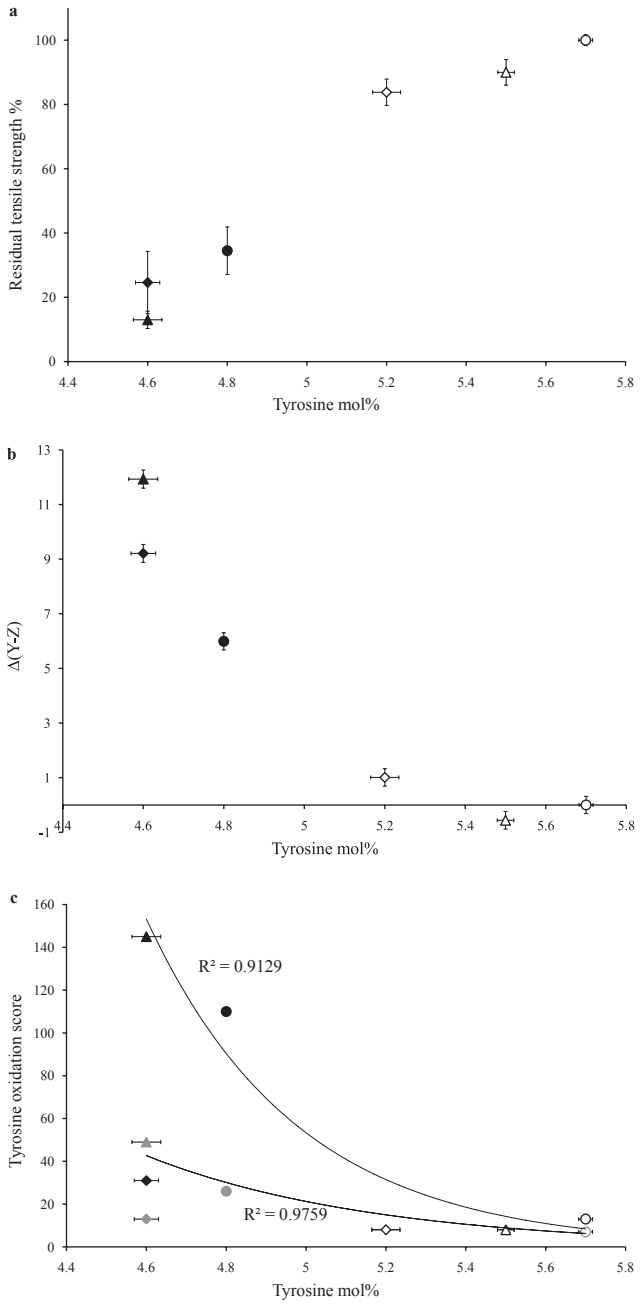

Figure 4. Correlation between: (a) tensile strength and tyrosine content, (b) yellowing and tyrosine content and (c) score of tyrosine oxidation products and tyrosine content of unaged samples (open symbols) and aged samples (solid symbols) for unweighted silk (circle), pink tin-weighted silk (triangle) and dynamite tin-weighted silk (diamond). The gray symbols represent the p scores and the black symbols the P scores.

However, despite loss in tyrosine content in the dynamite tin-weighted silk, few oxidized peptides are observed, resulting in an underestimated score of oxidation. The overall decrease in identified peptides after UV irradiation may be indicative of the formation of high levels of protein cross-linking. For instance, the formation of dityrosine is one type of cross-linking that could be responsible for the loss of performance during chymotryptic digestion as it is known for its high resistance to proteolysis (47), as well as to increase structural strength. The higher strength of the dynamite tin-weighted sample over the pink tin-weighted sample is another indication that the former fabric might contain a higher proportion of protein–protein cross-linking.

Acknowledgements—This work was supported by a Marie Curie International Outgoing Fellowship (PIOF-GA-2009-236425) between the University of York, UK and AgResearch, NZ. We gratefully acknowledge Pr. Matthew Collins for its useful suggestions and review of this manuscript. PW thanks his former colleagues at the Textile Conservation Centre, Winchester.

SUPPORTING INFORMATION

Additional Supporting Information may be found in the online version of this article:

Table S1. All identified peptides in unaged silks.

Table S2. All identified peptides in aged silks.

Please note: Wiley-Blackwell is not responsible for the content or functionality of any supporting information supplied by the authors. Any queries (other than missing material) should be directed to the corresponding author for the article.

REFERENCES

1. Currie, R. (2001) Silk. In *Silk, Mohair, Cashmere and other Luxury Fibres* (Edited by R. R. Franck), pp. 1–67. Woodhead Publishing Limited, Cambride, England.
2. Federico, G. (1996) An econometric model of world silk production, 1870–1914. *Explor. Econ. Hist.* **33**, 250–274.
3. Becker, M. A., Y. Magoshi, T. Sakai and N. C. Tuross (1997) Chemical and physical properties of old silk fabrics. *Stud. Conserv.* **42**, 27–37.
4. Becker, M. A., P. Willman and N. C. Tuross (1995) The U.S. First ladies gowns: a biochemical study of silk preservation. *J. Am. Inst. Conserv.* **34**, 141–152.
5. Pérez-Rigueiro, J., M. Elices, J. Llorca and C. Viney (2002) Effect of degumming on the tensile properties of silkworm (*Bombyx mori*) silk fiber. *J. Appl. Polym. Sci.* **84**, 1431–1437.
6. Garside, P., S. Lahlil and P. Wyeth (2005) Characterization of historic silk by polarized attenuated total reflectance fourier transform infrared spectroscopy for informed conservation. *Appl. Spectrosc.* **59**, 1242–1247.
7. Garside, P., P. Wyeth and X. Zhang (2010) Understanding the ageing behaviour of nineteenth and twentieth century tin-weighted silks. *J. Inst. Conserv.* **33**, 179–193.
8. Garside, P., P. Wyeth and X. Zhang (2010) The inherent acidic characteristics of silk, part II-weighted silks. *E-Pres. Sci.* **7**, 126–131.
9. Kim, J. and P. Wyeth (2009) Towards a routine methodology for assessing the condition of historic silk. *E-Pres. Sci.* **6**, 60–67.
10. Miller, J. E. and B. M. Reagan (1989) Degradation in weighted and unweighted historic silks. *J. Am. Inst. Conserv.* **28**, 97–115.
11. Garside, P. and P. Wyeth (2007) Crystallinity and degradation of silk: correlations between analytical signatures and physical condition on ageing. *Appl. Phys. A* **89**, 871–876.
12. Wyeth, P. (2005) Signatures of ageing: correlations with behaviour. In *Scientific Analysis of Ancient and Historic Textiles: Informing Preservation, Display and Interpretation* (Edited by P. Wyeth and R. Janaway), pp. 137–142. Archetype Publications, London.
13. Zhang, X., I. Vanden Berghe and P. Wyeth (2011) Heat and moisture promoted deterioration of raw silk estimated by amino acid analysis. *J. Cult. Herit.* **12**, 408–411.
14. Dyer, J. M., S. D. Bringans and W. G. Bryson (2006) Characterisation of photo-oxidation products within photoyellowed wool proteins: tryptophan and tyrosin derived chromophores. *Photochem. Photobiol. Sci.* **5**, 698–706.

15. Dyer, J. M., S. D. Bringans and W. G. Bryson (2006) Determination of photo-oxidation products within photoyellowed bleached wool proteins. *Photochem. Photobiol.* **82**, 551–557.
16. Dyer, J. M., J. E. Plowman, G. L. Krsinic, S. Deb-Choudhury, H. Koehn, K. R. Millington and S. Clerens (2010) Proteomic evaluation and location of UVB-induced photo-oxidation in wool. *J. Photochem. Photobiol., B* **98**, 118–127.
17. Dyer, J. M. (2010) Protein photo-oxidative damage-consequences, characterisation and control. In *Photobiology: Principles, Applications and Effects* (Edited by L. N. Collignon and C. B. Normand), pp. 91–113. Nova Science Publishers, Inc., Hauppauge, New York.
18. Smith, G. J. (1995) New trends in photobiology (invited review). photodegradation of keratin and other structural proteins. *J. Photochem. Photobiol., B* **18**, 7–198.
19. Zhang, P., Y. Aso, K. Yamamoto, Y. Banno, Y. Wang, K. Tsuchida, Y. Kawaguchi and H. Fujii (2006) Proteome analysis of silk gland proteins from the silkworm, *Bombyx mori. Proteomics* **6**, 2586–2599.
20. Jin, H.-J. and D. L. Kaplan (2003) Mechanism of silk processing in insects and spiders. *Nature* **424**, 1057–1061.
21. Marsh, R. E., R. B. Corey and L. Pauling (1955) An investigation of the structure of silk fibroin. *Biochim. Biophys. Acta* **16**, 1–34.
22. Yamaguchi, K., Y. Kikuchi, T. Takagi, A. Kikuchi, F. Oyama, K. Shimura and S. Mizuno (1989) Primary structure of the silk fibroin light chain determined by cDNA sequencing and peptide analysis. *J. Mol. Biol.* **210**, 127–139.
23. Mita, K., S. Ichimura and T. C. James (1994) Highly repetitive structure and its organization of the silk fibroin gene. *J. Mol. Evol.* **38**, 583–592.
24. Zhou, C.-Z., F. Confalonieri, N. Medina, Y. Zivanovic, C. Esnault, T. Yang, M. Jacquet, J. Janin, M. Duguet, R. Perasso and Z.-G. Li (2000) Fine organization of *Bombyx mori* fibroin heavy chain gene. *Nucleic Acids Res.* **28**, 2413–2419.
25. Xia, Q., Z. Zhou, C. Lu, D. Cheng, F. Dai, B. Li, P. Zhao, X. Zha, T. Cheng, C. Chai, G. Pan, J. Xu, C. Liu, Y. Lin, J. Qian, Y. Hou, Z. Wu, G. Li, M. Pan, C. Li, Y. Shen, X. Lan, L. Yuan, T. Li, H. Xu, G. Yang, Y. Wan, Y. Zhu, M. Yu, W. Shen, D. Wu, Z. Xiang, J. Yu, J. Wang, R. Li, J. Shi, H. Li, G. Li, J. Su, X. Wang, G. Li, Z. Zhang, Q. Wu, J. Li, Q. Zhang, N. Wei, J. Xu, H. Sun, L. Dong, D. Liu, S. Zhao, X. Zhao, Q. Meng, F. Lan, X. Huang, Y. Li, L. Fang, C. Li, D. Li, Y. Sun, Z. Zhang, Z. Yang, Y. Huang, Y. Xi, Q. Qi, D. He, H. Huang, X. Zhang, Z. Wang, W. Li, Y. Cao, Y. Yu, H. Yu, J. Li, J. Ye, H. Chen, Y. Zhou, B. Liu, J. Wang, J. Ye, H. Ji, S. Li, P. Ni, J. Zhang, Y. Zhang, H. Zheng, B. Mao, W. Wang, C. Ye, S. Li, J. Wang, G. K.-S. Wong and H. Yang (2004) A draft sequence for the genome of the domesticated silkworm (*Bombyx mori*). *Science* **306**, 1937–1940.
26. Mita, K., M. Kasahara, S. Sasaki, Y. Nagayasu, T. Yamada, H. Kanamori, N. Namiki, M. Kitagawa, H. Yamashita, Y. Yasukochi, K. Kadono-Okuda, K. Yamamoto, M. Ajimura, G. Ravikumar, M. Shimomura, Y. Nagamura, T. Shin-i, H. Abe, T. Shimada, S. Morishita and T. Sasaki (2004) The genome sequence of silkworm, *Bombyx mori. DNA Res.* **11**, 27–35.
27. Zhou, Z., H. Yang and B.-x. Zhong (2008) From genome to proteome: great progress in the domesticated silkworm (*Bombyx mori L.*). *Acta Biochim. Biophys. Sin.* **40**, 601–611.
28. Li, X.-h., X.-f. Wu, W.-f. Yue, J.-m. Liu, G.-l. Li and Y.-g. Miao (2006) Proteomic analysis of the silkworm (*Bombyx mori L.*) hemolymph during developmental stage. *J. Proteome Res.* **5**, 2809–2814.
29. Wu, X.-f., X.-h. Li, W.-f. Yue, B. Roy, G.-l. Li, J.-m. Liu, B.-x. Zhong, Q.-k. Gao, W. C. C. David and Y.-g. Miao (2009) Proteomic identification of the silkworm (*Bombyx mori* L.) prothoracic glands during the fifth instar stage. *Bioscience Rep.* **29**, 121–129.
30. Jia, S.-h., M.-w. Li, B. Zhou, W.-b. Liu, Y. Zhang, X.-x. Miao, R. Zeng and Y.-p. Huang (2007) Proteomic analysis of silk gland programmed cell death during metamorphosis of the silkworm *Bombyx mori. J. Proteome Res.* **6**, 3003–3010.
31. Chen, W.-Q., H. Priewalder, J. P. P. John and G. Lubec (2010) Silk cocoon of *Bombyx mori*: proteins and posttranslational modifications—heavy phosphorylation and evidence for lysine-mediated cross links. *Proteomics* **10**, 369–379.
32. Zhang, P., K. Yamamoto, Y. Aso, Y. Banno, D. Sakano, Y. Wang and H. Fujii (2005) Proteomic studies of isoforms of the P25 component of *Bombyx mori* fibroin. *Biosci. Biotechnol. Biochem.* **69**, 2086–2093.
33. Asakura, T., R. Sugino, J. Yao, H. Takashima and R. Kishore (2002) Comparative structure analysis of tyrosine and valine residues in unprocessed silk fibroin (silk I) and in the processed silk fiber (Silk II) from *Bombyx mori* using solid-state ^{13}C,^{15}N, and ^{2}H NMR. *Biochemistry* **41**, 4415–4424.
34. Ha, S.-W., H. S. Gracz, A. E. Tonelli and S. M. Hudson (2005) Structural study of irregular amino acid sequences in the heavy chain of *Bombyx mori* silk fibroin. *Biomacromolecules* **6**, 2563–2569.
35. Mondal, M., K. Trivedy and S. Nirmal Kumar (2007) The silk proteins, sericin and fibroin in silkworm, *Bombyx mori* Linn.,-a review. *Caspian J. Env. Sci.* **5**, 63–76.
36. Tanaka, K., N. Kajiyama, K. Ishikura, S. Waga, A. Kikuchi, K. Ohtomo, T. Takagi and S. Mizuno (1999) Determination of the site of disulfide linkage between heavy and light chains of silk fibroin produced by *Bombyx mori. Biochim. Biophys. Acta* **1432**, 92–103.
37. Inoue, S., K. Tanaka, F. Arisaka, S. Kimura, K. Ohtomo and S. Mizuno (2000) Silk fibroin of *Bombyx mori* is secreted, assembling a high molecular mass elementary unit consisting of H-chain, L-chain, and P25, with a 6:6:1 molar ratio. *J. Biol. Chem.* **275**, 40517–40528.
38. Sashina, E. S., A. M. Bochek, N. P. Novoselov and D. A. Kirichenko (2006) Structure and solubility of natural silk fibroin. *Russ. J. Appl. Chem.* **79**, 869–876.
39. Ajisawa, A. (1998) Dissolution of silk fibroin with calcium chloride/ethanol aqueous solution. *J. Seric. Sci. Jpn* **67**, 91–94.
40. Li, M., M. Ogiso and N. Minoura (2003) Enzymatic degradation behaviour of porous silk fibroin sheets. *Biomaterials* **24**, 357–365.
41. Miyaguchi, Y. and J. Hu (2005) Physicochemical properties of silk fibroin after solubilization using calcium chloride with or without ethanol. *Food Sci. Technol. Res.* **11**, 37–42.
42. Yamada, H., H. Nakao, Y. Takasu and K. Tsubouchi (2001) Preparation of undegraded native molecular fibroin solution from silkworm cocoons. *Mat. Sci. Eng. C* **14**, 41–46.
43. Dyer, J. M., C. D. Cornellison, S. D. Bringans, G. Maurdev and K. R. Millington (2008) The photoyellowing of stilbene-derived fluorescent whitening agents-mass spectrometric characterization of yellow photoproducts. *Photochem. Photobiol.* **84**, 145–153.
44. Grosvenor, A. J., J. D. Morton and J. M. Dyer (2010) Profiling of residue-level photo-oxidative damage in peptides. *Amino Acids* **39**, 285–296.
45. Arai, T., G. Freddi, R. Innocenti and M. Tsukada (2004) Biodegradation of *Bombyx mori* silk fibroin fibers and films. *J. Appl. Polym. Sci.* **91**, 2383–2390.
46. Dyer, J. M., S. Clerens, C. D. Cornellison, C. J. Murphy, G. Maurdev and K. R. Millington (2009) Photoproducts formed in the photoyellowing of collagen in the presence of a fluorescent whitening agent. *Photochem. Photobiol.* **85**, 1314–1321.
47. Atwood, C. S., G. Perry, H. Zeng, Y. Kato, W. D. Jones, K.-Q. Ling, X. Huang, R. D. Moir, D. Wang, L. M. Sayre, M. A. Smith, S. G. Chen and A. I. Bush (2004) Copper mediates dityrosine cross-linking of Alzheimer's amyloid-β. *Biochemistry* **43**, 560–568.